ACS Partner Journal

ACCOUNTS of materials research

pubs.acs.org/amrcda Article

Durable Super-repellent Surfaces: From Solid–Liquid Interaction to Applications

Fanfei Yu, Dehui Wang, Jinlong Yang, Wenluan Zhang, and Xu Deng*

Cite This: *Acc. Mater. Res.* 2021, 2, 920–932 Read Online

ACCESS | Metrics & More | Article Recommendations

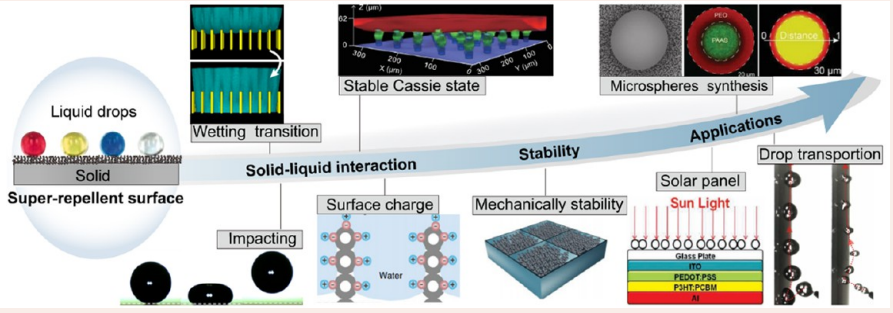

CONSPECTUS: A super-repellent surface is a type of liquid-repellency material that allows for various liquid drops to bead up, roll off, or even bounce back. Known for its ability to remain dry, perform self-cleaning, and have a low adhesion, a super-repellent surface presents great advantages in a number of applications. These include antifogging, anti-icing, oil/water separation, and fluid drag reduction. To fend off the liquids or drops, super-repellent surfaces combine the merits of surface chemistry and physical structure. By taking advantage of a low surface energy to prevent liquid from spreading, the super-repellent surfaces utilize the micronano structure to provide a framework that confines the solid–liquid interactions. Compared to beading up the drop of water, the repellence of liquid with low surface tension requires the subtle design of surface structure to resist the wetting of liquids. However, the inherent instabilities of the fragile micronano structure of super-repellent surfaces and solid–liquid interactions further make the fabrication of super-repellent surfaces complex to withstand dynamic environments (friction or wear) during application. In addition, the transparency and thermal stability of super-repellent surfaces are also the restrictive factors in some special application scenarios. To solve these challenges, durable super-repellent surfaces that can repel various liquids, possess robust mechanical and thermal stability, and show high transparency have been explored extensively in recent years.

In this Account, we systematically review our recent efforts to promote the super-repellent surfaces for real-world applications. Super-repellent surfaces that exhibit excellent resistance to various liquids, including liquids with low surface tension or high viscosity, were subtly designed and fabricated in some manner. Considering the stability of the wetting state at the solid–liquid interface, we established an evaluation system that includes highly curved surfaces and high Laplace-pressure conditions. To further perfect the wetting mechanism at the solid–liquid interactions, the dynamic wettability of super-repellent surfaces regulated by surface charge enrichment that was generated from solid–liquid interface separation was investigated. To resolve the bottleneck problem of the mechanical stability of super-repellent surfaces in real-world applications, a new decoupling material design mechanism was proposed, with a nanostructure that maintains water repellency and a microstructure providing durability. On the basis of the performance of the liquid-repellency, transparency, and mechanical and thermal stability of the super-repellent surfaces, a series of applications were demonstrated, such as microsphere synthesis, drop transportation and manipulation, and self-cleaning solar panels. Finally, a concise summary of this Account, including challenges and opportunities in super-repellent materials, has been provided. This research provides important guidance on solid–liquid interactions for the design of functional super-repellent surfaces and plays an important role in promoting large-scale industrial applications.

1. INTRODUCTION

When liquids or drops touch a surface, they generate solid–liquid interfaces, where surface wetting phenomena, i.e., liquid spreading and repellency, occur. The wettability, which is a unique feature of the material surface, controls the surface performance, such as self-cleaning,[1,2] antifogging,[3] anti-icing,[4,5] oil/water separation,[6] and fluid drag reduction.[7,8] An under-

Received: July 1, 2021
Published: September 15, 2021

https://doi.org/10.1021/accountsmr.1c00147
Acc. Mater. Res. 2021, 2, 920–932

standing and regulation of the solid−liquid interaction for the development of functional surfaces with special wettability, which can withstand the challenges of complex application environments, has become a key issue in surface science and engineering.[9]

Since the self-cleaning effect of the lotus leaf was revealed,[10] biological surfaces with liquid repellency have attracted extensive attention.[11,12] These super-repellent surfaces obtain their properties from their fine texture. Super-repellent surfaces have been reported that incorporate the principle of wetting, such as superhydrophobic and superoleophobic surfaces.[13−19] However, challenges arise when these artificial super-repellent surfaces are used to repel, for example, sewage or oil−water mixtures. For such liquids, superamphiphobic surfaces,[20] namely, surfaces that repel both water and low-surface-tension liquids, are desired. Nonaqueous liquids introduce complications into the liquid−solid interactions, which require systematic studies from the wetting mechanism to real-world applications. For example, evaluation standards for the wetting state stability and especially for surfaces with highly curved structures or under a high liquid impacting pressure are required; the influence of the surface charge enrichment effect on the surface wetting behavior during solid−liquid interface contact and the separation process must be understood. The instability of super-repellent materials and the solid−liquid interaction further complicate applications in terms of wear resistance, water impact resistance, mechanical stability, and chemical and thermal durability.[14,21] Of these stabilities, the mechanical stability of the surface mirco/nanostructure is the biggest obstacle to the widespread application of super-repellent surfaces.

In recent years, our group has focused on an exploration of the basic physical and chemical principles as related to solid−liquid interfaces. We have targeted the aforementioned problems of super-repellent surfaces, carried out research on the wetting mechanism and functional stability of super-repellent materials, and aimed to address the practical applications, as shown in Figure 1. We started with the wetting mechanism of super-repellent surfaces. In this part, we discuss the design principle and fabrication of the super-repellent surface, the static and dynamic wetting state of the solid−liquid interface, and the influence of the surface charge enrichment effect on the wettability at the solid−liquid interface. On the basis of the functional stability of super-repellent materials in practical applications, we provide a perspective on super-repellent materials: how to divide the liquid repellency and mechanical properties of the material into two different length scales to strengthen the super-repellent properties and stabilities simultaneously. We demonstrated the application of super-repellent surfaces in microsphere synthesis, drop transportation, and self-cleaning solar cells. Meanwhile, at the end of this Account, we consider the opportunities and challenges faced by super-repellent materials.

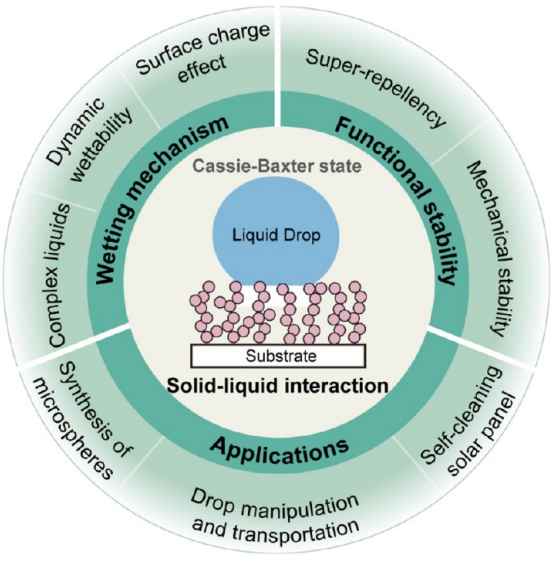

Figure 1. Overview of our recent progress in super-repellent surfaces.

2. WETTING MECHANISM AT THE SOLID−LIQUID INTERFACE

2.1. Key Concepts for the Wetting State on Material Surfaces

The contact angle (CA) at the solid−liquid−gas three-phase contact line has been used as a key parameter to characterize the wettability of material surfaces. Pioneering works have explained such solid−liquid interactions by a wetting equation. On a smooth ideal solid surface (Figure 2a), the equilibrium wetting state of a drop is described by Young's equation[22]

$$\gamma_{lv} \cos \theta_Y = \gamma_{sv} - \gamma_{ls} \quad (1)$$

where γ_{lv}, γ_{sv}, and γ_{ls} are the surface tensions for the liquid−vapor, solid−vapor, and liquid−solid interfaces, respectively, and θ_Y represents the intrinsic contact angle. The surface roughness changes the measured contact angles in contrast to the smooth surfaces. In later developments, two distinct wetting modes were established for an improved understanding of nonideal surfaces. When a drop forms a continuous solid−liquid interface (Figure 2b), the apparent contact angle (θ^*) is described by the Wenzel equation[23]

$$\cos \theta_W^* = r \cos \theta_Y \quad (2)$$

where r is the roughness factor of the surface, which is defined as the ratio of the actual surface area to the projected surface area of the solid surface. When the drop is suspended on a composite interface that is composed of a surface structure and a trapped air cushion in global thermodynamic equilibrium (Figure 2c), θ^* is described by the Cassie−Baxter equation[24]

$$\cos \theta_C^* = \varphi_S(\cos \theta_Y + 1) - 1 \quad (3)$$

where φ_s is the solid−liquid contact area of the surface. A high θ^* indicates that drops exist on a solid surface with a low solid−liquid interface adhesion because of the small solid−liquid contact area, which is a featured characteristic of super-repellent surfaces. It should be noted that the apparent contact angle θ^* by itself does not determine the rolling or moving behavior of a drop on the surface. A drop sitting on a rough surface exhibits different contact angles in two extreme ranges caused by pinning. The maximum observed angle is the advancing contact angle θ_{adv}, and the minimum corresponding angle is the receding contact angle θ_{rec}. For a moving drop, the mobility also depends on the variation in dynamic contact angle, i.e., the contact angle hysteresis $\Delta\theta = \theta_{adv} - \theta_{rec}$, as shown in Figure 2d. A surface with a high static θ^* and a low $\Delta\theta$ enables liquid drops to roll off easily. When the θ^* for water or oils exceeds 150° and $\Delta\theta \leq 10°$, we describe the super-repellent surface as superhydrophobic or superoleophobic, respectively. When the super-repellent surface

https://doi.org/10.1021/accountsmr.1c00147
Acc. Mater. Res. 2021, 2, 920−932

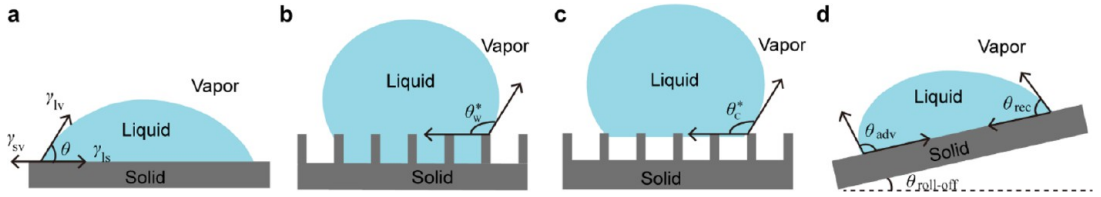

Figure 2. Wetting modes at the solid–liquid interface. (a) A drop deposited on an ideal solid surface, showing the intrinsic contact angle (CA) of the drop (θ_Y). (b, c) A drop sitting on a rough solid surface, showing the apparent CA (θ^*) in the Wenzel state and the Cassie–Baxter state, respectively. (d) Contact angle hysteresis $\Delta\theta$, which is defined as the difference between θ_{adv} and θ_{rec}, and the roll-off angle ($\theta_{roll\text{-}off}$).

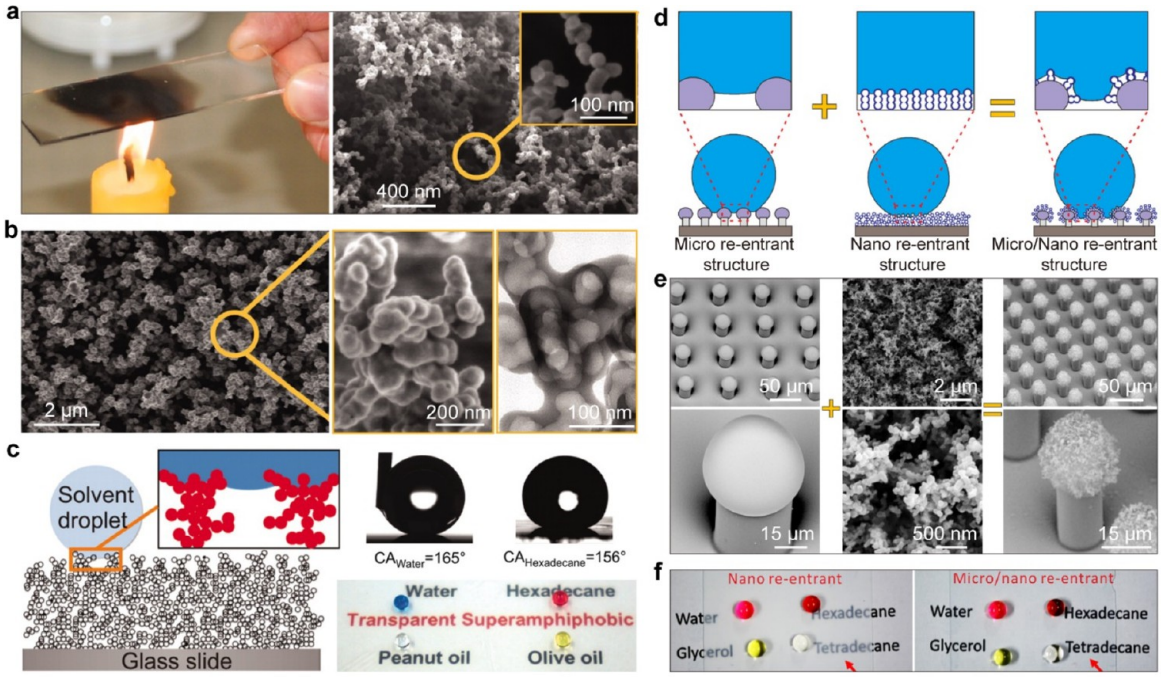

Figure 3. Design and fabrication of superamphiphobic surfaces for repelling various liquids. (a) Deposition method and scanning electron microscope (SEM) morphology of the candle-soot layer. The inset is a high-resolution SEM image showing the details of the soot composed of carbon particles. (b) SEM images of the hollow nanomicro composite structure of silica spheres. The insets show the high-resolution SEM and TEM images. (c) Superrepellency performance of the candle-soot-templated nanomicro structure. (d) Design strategy of the micro/nano re-entrant-coordinated superamphiphobic surface. (e) SEM images showing the micro re-entrant, the nano re-entrant, and the micro/nano re-entrant-coordinated structure. (f) Optical transparency and repellency performance of the nano re-entrant surface and the micro/nano re-entrant-coordinated surface. (a–c) Reproduced with permission from ref 20. Copyright 2012 American Association for Advancement Science. (d–f) Reproduced with permission from ref 27. Copyright 2019 American Chemical Society.

meets the criteria for both water and oils, we use the term superamphiphobic to describe the surface wettability.

2.2. Design and Fabrication of Surfaces for Repelling Low-Surface-Tension Liquids

For water repellency, two essential parameters, namely, a low surface energy and roughness, make the surface superhydrophobic. However, liquids with a low surface tension spread on a solid surface despite its superhydrophobicity because of the weak cohesion between liquid molecules,[18] which induces surface wetting. To achieve the repellency of low-surface-energy liquid, the chemical composition and roughened texture together with a re-entrant surface curvature are all imperative to maintaining the liquid advancing contact line in a metastable state with captured air underneath.[18,25] The interaction effect among these three factors complicates the superamphiphobic surface design and fabrication to repel liquids. Inspired by the fractal-like candle soot that repels water drops, we engineered a candle-soot-templated transparent superamphiphobic material with water and oil repellency.[20] The re-entrant template was made from nanospherical carbon particles, which were generated from the incomplete combustion of low-cost alkane mixtures and self-assembled into a fractal-like microscale network because of the constrained diffusion during combustion (Figure 3a). To reinforce the mechanical strength of the as-prepared coating, the candle-soot layer was covered with a silica shell by employing the chemical vapor deposition of tetraethoxysilane that is catalyzed by ammonia. In addition, the surface transparency was achieved by calcining the carbon core and generating a hollow nanomicro composite silicon sphere structure (Figure 3b). After dealing with a low-surface-energy substance, the resulting porous structure exhibited excellent repellency to water and low-surface-energy liquid drops, such as hexadecane (27.5 mN/m) and peanut oil (34.5 mN/m), as shown in Figure 3c. By taking advantage of the simple preparation process, such transparent superamphiphobic surfaces exhibit excellent liquid repellency and resistance during drop impact at high impacting energy. This method can be applied to a variety of substrates, such as silicon wafers, aluminum, stainless steel, and copper.[20] Apart

https://doi.org/10.1021/accountsmr.1c00147
Acc. Mater. Res. 2021, 2, 920–932

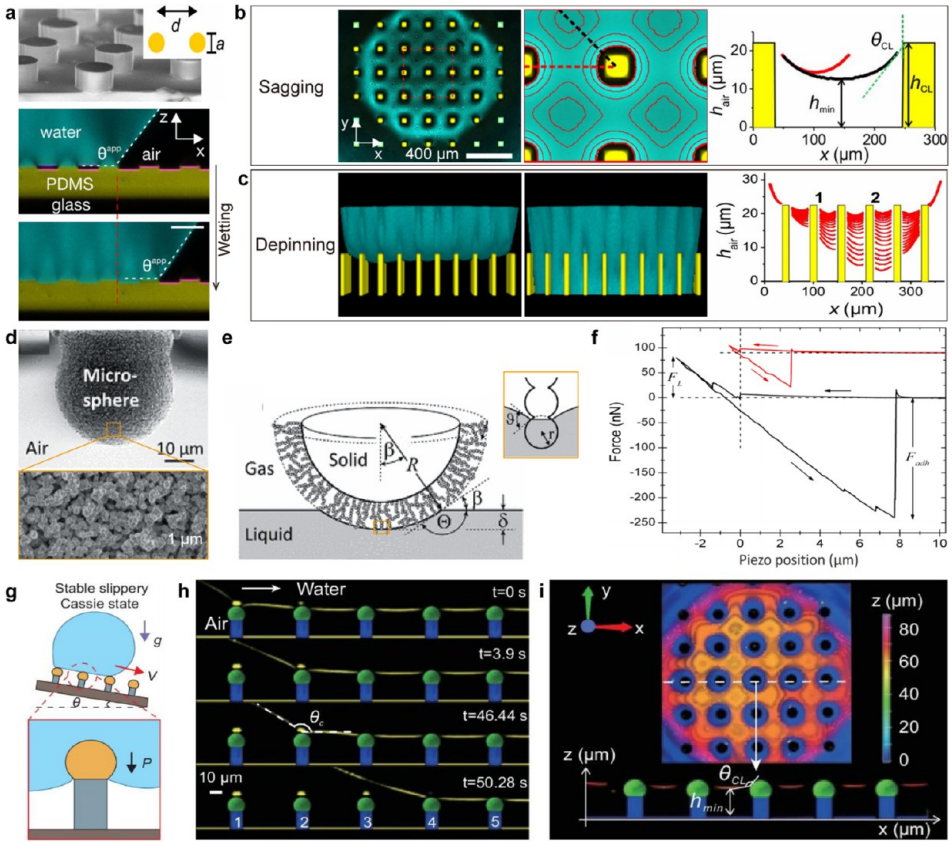

Figure 4. Stability of the wetting state at the solid−liquid interface. (a) Cassie-to-Wenzel transition of a drop on a micropillar structured surface during the process of evaporation captured by confocal microscopy. (b) Cassie-to-Wenzel transition in the sagging regime. (c) Cassie−Wenzel transition in the depinning regime. (d) SEM image of a superamphiphobically coated microsphere. (e) Schematic diagram of the superamphiphobic microsphere just in contact with the surface of the liquid. (f) Measurement of the force versus distance curves during a superamphiphobic microsphere interacting with a liquid drop. (g) Design of a slippery stable Cassie state by a Salvinia-like slippery surface (SSS). (h) Lateral mobility: confocal image showing the vertical cross-section on the receding side of a water drop during the moving process. (i) Vertical stability of the Cassie state on the SSS during evaporation: confocal image of the reflection from the water/air interface when a drop is deposited on the surface. (d−f) Reproduced with permission from ref 30. Copyright 2014 American Physical Society.

from the superamphiphobic surface relying on stringed nanoparticles to make re-entrant geometries, recent research also showed a new type of superamphiphobic surface composed of hedgehog microparticles.[26] Such a hedgehog surface exhibits high superamphiphobicity by combining the micro re-entrant textures surrounded by nanoneedle structures.

Generally, the existence of the surface texture influences the light absorption, reflection, and scattering. High surface transparency is often achieved at the expense of nanostructures. To further optimize the surface liquid repellency and transparency, a model design of the hierarchical structure was proposed by combining the nano and micro re-entrant structures,[27] as shown in Figure 3d. The nano re-entrant structure contributed to reducing the solid−liquid adhesion, and the micro re-entrant structure was responsible for structuring homogeneousness to ensure the high transparency of the surface. By introducing the optimized micropillar pattern structure and aggregated candle-soot-templated silica nanostructures (Figure 3e), the obtained micronano re-entrant-coordinated superamphiphobic surface attained a nano and micro re-entrant structure without losing its original character in liquid repellency and structure uniformity. Compared with the candle-soot-templated silica nanostructure, the existence of an optimized micropillar pattern structure reduced the solid−liquid contact fraction and ensured the microscale uniformity of the structure. The resulting surface presented an ultralow solid−liquid adhesion to low-surface-energy or high-viscosity liquids and excellent transparency, as shown in Figure 3f. Besides, it should be noted that although the re-entrant structures are well adopted to maintain super-repellency, the wetting robustness is still poor. Recent research has also shown that one elegant approach to further maintaining the robust wetting property is to introduce multiple-layered re-entrant structures to resist wetting in a stepwise mode.[28]

2.3. Stability of the Wetting State at the Solid−Liquid Interface

The remarkable liquid-repellent property of the materials originates from the engineered surface structure that entraps air pockets beneath the drop and yields the Cassie state. However, the high-energy Cassie state is unstable. It competes with the Wenzel state in which the liquid wets the substrate fully at a favorable low-energy state. Such a transition in these two wetting states develops in two main ways, namely, sagging and depinning of the liquid at the solid−liquid−vapor three-phase interface. In the sagging mechanism, the meniscus liquid−vapor interface suspended between the structural elements droops continuously and contacts the base, and then the Cassie-to-Wenzel transition occurs. In the depinning mechanism, a completely wetting Wenzel state is developed when the three-phase contact line unpins from the rim of the structural element

https://doi.org/10.1021/accountsmr.1c00147
Acc. Mater. Res. 2021, 2, 920−932

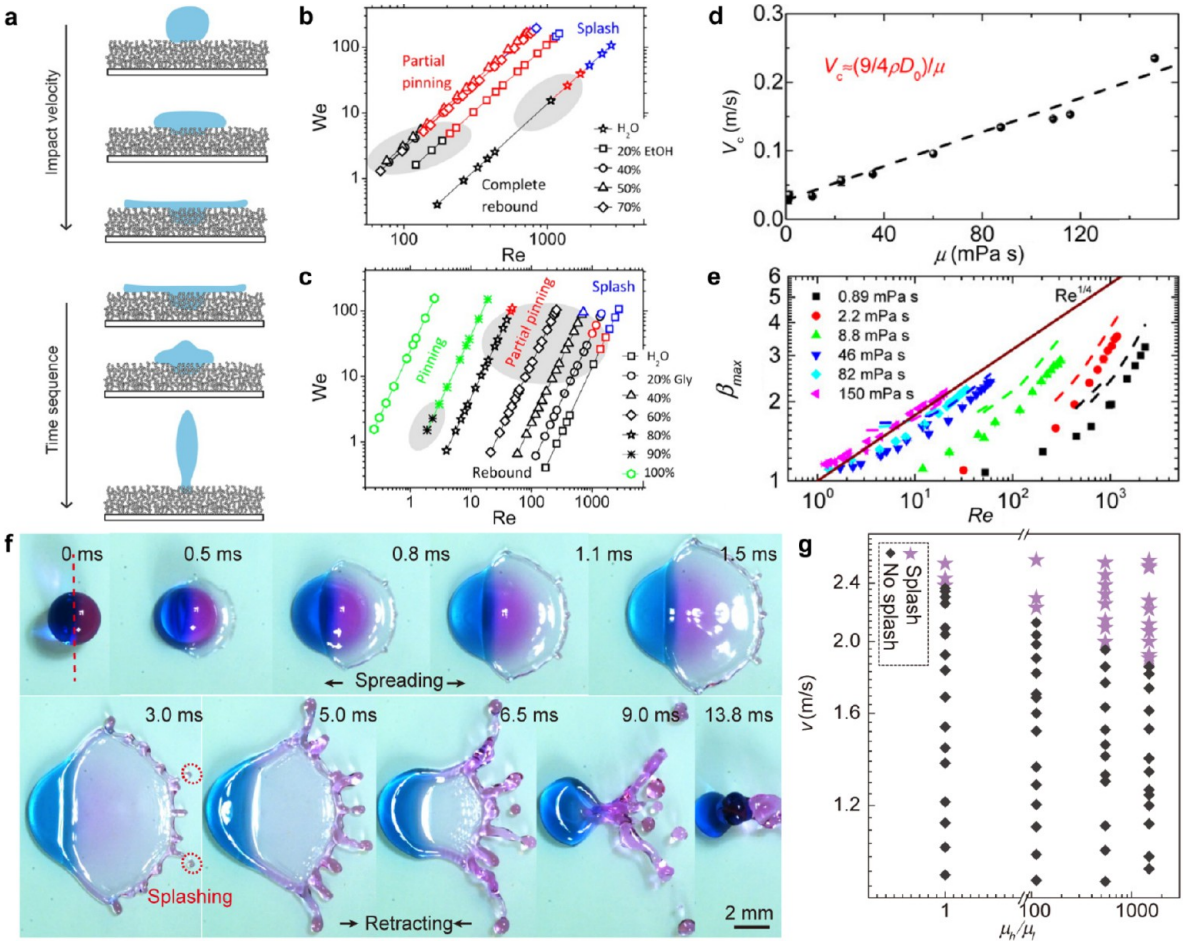

Figure 5. Dynamic wettability of the super-repellent materials during drop impact. (a) Sketch of the wetting state during drop impact on a superamphiphobic surface. (b) Influence of liquid surface tension on impacting outcomes and the wetting state. (c) Influence of liquid viscosity on impacting outcomes and the wetting state. (d) Threshold impacting velocity V_c for the impacting drop rebound in response to the liquid viscosity μ. (e) Maximum spreading factors as a function of *Re* for liquid with different viscosities. (f) Prompting splash during drop impact induced by a local viscosity increase. (g) Phase diagram of impacting velocity v along with the viscosity ratio μ_h/μ_l of the drop. (a–c) Reproduced with permission from ref 35. Copyright 2013 American Chemical Society. (d, e) Reproduced with permission from ref 36. Copyright 2017 American Chemical Society.

and slides down along the sidewall. To understand the underlying process of these two mechanisms, details of the impalement dynamics, including the temporal evolution of the thickness of the air cushion and the liquid–air meniscus, which induced the increment in Laplace pressure from evaporation, were monitored with sufficient spatial resolution by laser scanning confocal microscopy,[29] as shown in Figure 4a–c. Besides the impalement that is induced by an increase in Laplace pressure from evaporation, the effect of the curvature of the substrate on the wetting systems is rarely studied.

To quantify the dependence of wetting behavior on the curvature of the superamphiphobic surfaces, the adhesion force of a superamphiphobic coated microsphere and liquid was detected from colloidal probe spectroscopy by using microspheres with a radius R,[30] as shown in Figure 4d,e. The adhesion of superamphiphobically coated microspheres was read from force versus distance curves (Figure 4f). By measuring and analyzing the adhesion force between the microspheres and different liquids, the different microscopic and macroscopic contact angles that caused air entrapment were revealed. The curvature of the microspheres enlarged the possibility for liquids to impale the micronano structure of the superamphiphobic surfaces. Such surface-curvature-induced liquid wetting arises from the capillary pressure that is related to the liquid cavity around the particle. This indicates that the superamphiphobicity is curvature-correlated.[30] Research on the curvature-dependent superamphiphobicity provides guidance on the applications of super-repellent surfaces on small objects with a high curvature.

To achieve a stable Cassie state of liquid repellency, efforts have been made to stabilize the three-phase contact line by optimizing the structure morphology.[18,31,32] However, attempts to stabilize the vertical contact line sacrificed the lateral mobility of the contact line. To optimize the mobility of the contact line in both directions, a composite structure that is based on the superhydrophobic Cassie mode and the slippery mode was proposed.[33] It finally formed a slippery, stable Cassie state (Figure 4g). The structure stabilizes the contact line in the vertical direction by the increased energy barrier from the lubrication to the hydrophobic zone while the mobility of the contact line in the lateral direction was enhanced by the lubricant effect. The resultant composite surface presents the lateral mobility of the microscopic water/air contact line and the stability of the Cassie–Baxter wetting state, as shown in Figure 4h,i, respectively.

When the superamphiphobic surfaces meet incoming drops, i.e., the drop impact, the intensive dynamic interaction between the surface and drop complicates the stability of the wetting state. After impacting the surface, the drop spreads and retracts,

https://doi.org/10.1021/accountsmr.1c00147
Acc. Mater. Res. 2021, 2, 920–932

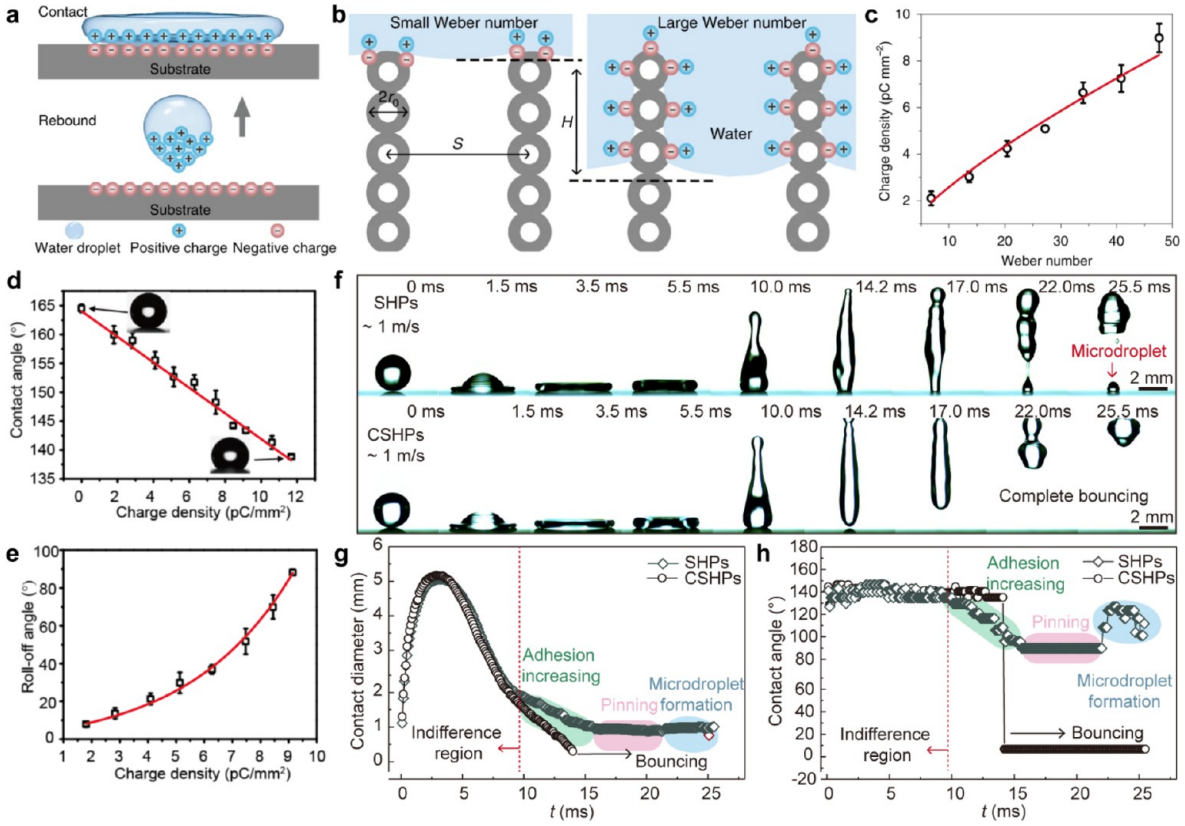

Figure 6. Influence of the surface charge accumulation effect on the wettability at the solid−liquid interface. (a) Charging process of a superamphiphobic surface during drop impingement. (b) Schematic diagram of the solid/liquid/vapor three-phase contact line during drop impact with different impact energy (*We*). (c) Influence of the *We* of the impacting drop on the charge density at the impacting area of the superamphiphobic surface. (d, e) Variation of the contact angle and roll-off angle for water along with the surface charge density, respectively. (f) Effect of surface charge generation on the dynamic behavior of the drop impact itself. Surface charge induced microdroplet formation during drop impact on SHPs, while the impact drop fully rebounded on conduct superhydrophobic surface (CSHPs). (g, h) Variation of the contact diameter and contact angle during drop impact on SHPs and CSHPs, respectively. (a−e) Reproduced with permission from ref 38. Copyright 2019 Springer Nature. (f, g) Reproduced with permission from ref 39. Copyright 2020 American Chemical Society.

as shown in Figure 5a. During the interaction, a local hydraulic pressure variation that was associated with the kinetic and interfacial energy transfer and viscous energy dissipation influences the composite solid−liquid−vapor interface strongly.[34] In comparison with a drop of water, the description of a nonpolar drop impact is more important because its impalement leads to a permanent failure of the Cassie state.[35] As shown in Figure 5b,c, the transition from complete rebound to partial pinning to splash was studied systematically by altering the initial impacting velocity (v), surface tension (γ), and viscosity (μ) of the impacting drop. The ratio of the drop's kinetic to surface energy or viscous energy diffusion was correlated to the dimensionless Weber number ($We \approx \rho v^2 D/\gamma$) and Reynolds number ($Re \approx \rho v D/\mu$), where ρ is the liquid density and D is the diameter of the impacting drop. At a low *We*, the drops rebound completely. The drop impales the micro/nanostructure beneath its initial impact position. By increasing *We*, the liquid impales the structure more deeply and presents partial pinning on the surface. In this regime, the wetting pressure of the impacting drop results in a critical wetting depth that goes beyond a viscosity and surface-tension-dependent threshold,[35] leading to the partial wetting state. Generally, the transition from complete rebound to partial pinning in the wetting state depends on the balance of wetting pressure, i.e., liquid entry pressure, and antiwetting pressure, i.e., depinning pressure. Partial pinning occurs when the critical wetting pressure goes beyond the antiwetting pressure. At sufficiently high *We*, the rim of the impacting drop breaks up and induces a splash.

An increase in liquid viscosity decelerates the impact process itself and induces lifting drops to rebound at a lower height with a lower frequency.[36] As shown in Figure 5d, the impacting velocity threshold of the full rebound of the drop on the superamphiphobic surface increases linearly with the increase in drop viscosity. This is because the kinetic energy of the impacting drop is dissipated by the internal viscosity of the liquid. High drop viscosity leads to more viscosity dissipation. Therefore, the energy available for drop rebound is reduced and the rebound speed is lowered. The maximum spreading diameter (D_{max}) plays an important role in characterizing the impacting outcomes. A model of maximum spreading factors ($\beta_{max} = D_{max}/D_0$) as a function of *Re* of the liquid with different viscosities was established (Figure 5e). Despite the uniform increase in drop viscosity that slows the impact and hinders the splash, the introduction of a partial high-viscosity phase onto a drop promotes the splashing during impact.[37] As shown in Figure 5f, when a glycerin drop was imposed on a water drop, the resulting drop, which was shaped into a Janus drop composed of a high viscosity part and low viscosity part, encounters splashing compared to a drop of water at the same impacting velocity. This is because the viscous stress that is applied by the low-viscosity water part propels the viscous glycerin part in the reverse

https://doi.org/10.1021/accountsmr.1c00147
Acc. Mater. Res. 2021, 2, 920−932

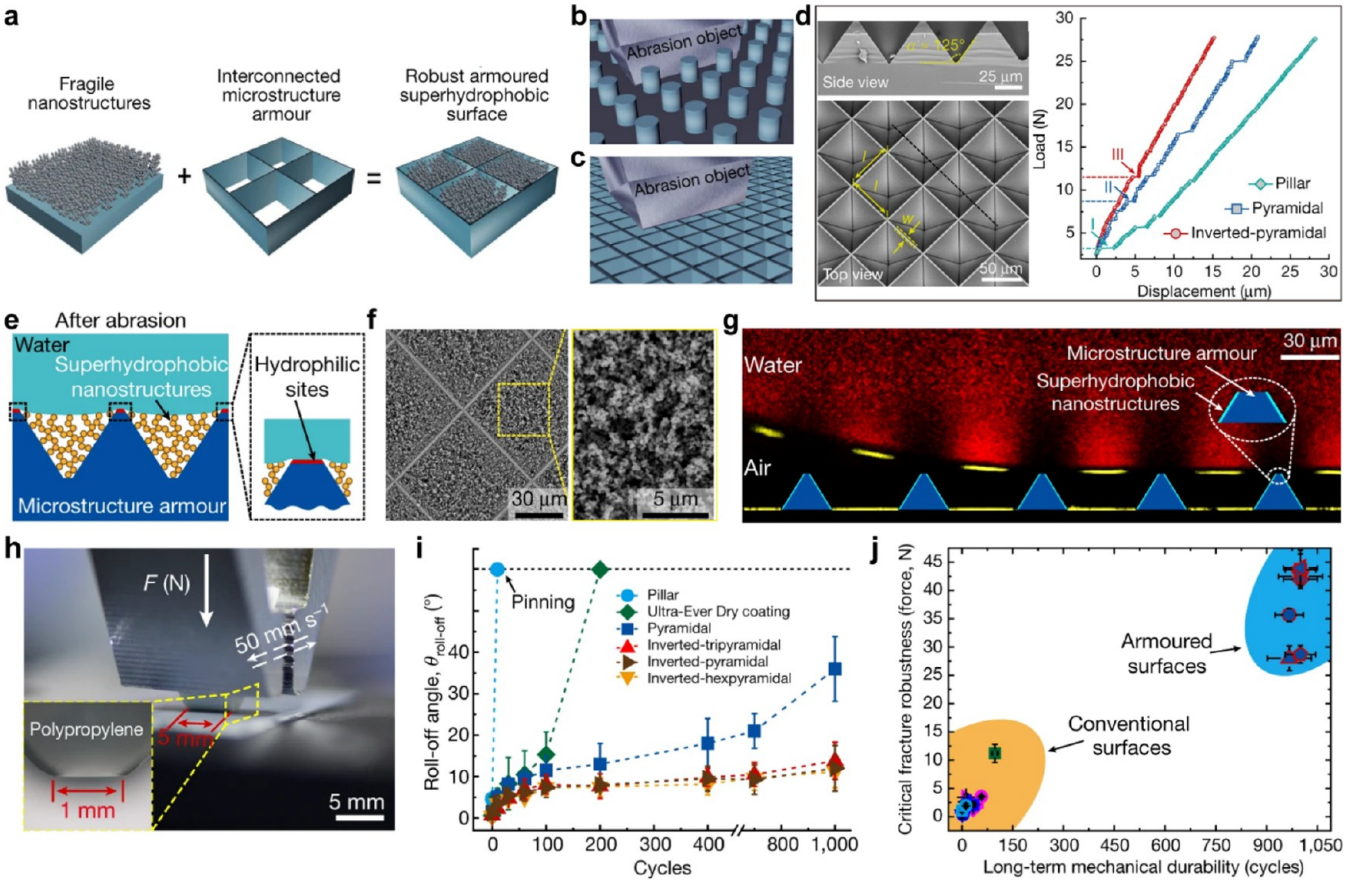

Figure 7. Robust superhydrophobic surface with superior mechanical stability. (a) Design principle to reinforce the superhydrophobic surface mechanical stability by armor. (b, c) Schematic diagrams present the comparison of abrasion damage to discrete and interconnected microstructures, respectively. (d) SEM images of the inverted-pyramidal interconnected microstructures on silicon, showing excellent mechanical performance compared to the pillar or pyramidal microstructures. (e, f) Schematic and SEM images of the armored superhydrophobic surface after abrasion. (g) Confocal microscopy image showing the stable Cassie state of a drop on the armored superhydrophobic surface after abrasion. (h) Snapshot of the linear abrasion configuration. (i) Linear abrasion cycles as a function of the roll-off angles for superhydrophobic surfaces with different microstructures. (j) Comparison of the long-term mechanical durability for an armored superhydrophobic surface and conventional surfaces. Reproduced with permission from ref 41. Copyright 2020 Springer Nature.

orientation. The spreading of the low-viscosity part and its rim instability were therefore promoted.[37] The threshold velocity of the splash can be regulated by varying the viscosity of the Janus drop, as shown in Figure 5g.

2.4. Influence of the Surface Charge Enrichment Effect on Wettability at the Solid−Liquid Interface

Surface charge exists at the solid−liquid or solid−gas interface and is generated by various physical/chemical processes, such as ion adsorption, protonation or deprotonation, and polarization. Our recent research found that surface charge is generated after a water drop impacts the superamphiphobic surface,[38] leaving the surface with a negative charge and the drop with a positive charge, as shown in Figure 6a. Although the mechanism of surface charge separation at the solid−liquid interface remains an open question, it may be explained by the counterion effect: counterions in the bare silica patches (Si−OH) with the superamphiphobic surface during drop impact are removed and leave SiO_x^-, whereas the water drop is protonated as H_3O^+. A large impacting energy gives rise to a high surface charge density because of the larger solid−liquid contact area that is available for surface charge generation (Figure 6b). Therefore, the surface charge density of the superamphiphobic surface can be regulated by the impacting energy (We), as shown in Figure 6b,c. The generation and density of the surface charge influence the wettability of the superamphiphobic surface, which is evaluated by the static CA (Figure 6d) and dynamic roll-off angle (Figure 6e). This is because the accumulated surface charges leads to a lower interfacial tension, which lowers the contact angle and increases the solid−liquid interface adhesion. It should be noted that since the accumulated surface charge stays on top of the surface, the stability of the superhydrophobic surface may not be affected, which can be reflected by the erasability of the surface charge and reversibility of the adhesion. Although the research on the charging mechanism of the solid−liquid contact is still limited, it is known that hydrophobic molecules, especially those with fluorine, are more conducive to the charge-separation phenomenon at the solid−liquid interface. Teflon, for example, can also be charged through water impact.

The generation of surface charge on the superamphiphobic surface affects the impacting dynamic behaviors itself due to the increase in surface adhesion.[39] In the contraction phase of the impacting process, an intense solid−liquid interaction comes into being between the impacting drop and the surface because of the generation of surface charge. The strong interaction leads to the failure of the complete rebound of the impacting drop on the superamphiphobic surface, while leaves a microdroplet on the impacting area, as shown in Figure 6f. The effect of surface

https://doi.org/10.1021/accountsmr.1c00147
Acc. Mater. Res. 2021, 2, 920−932

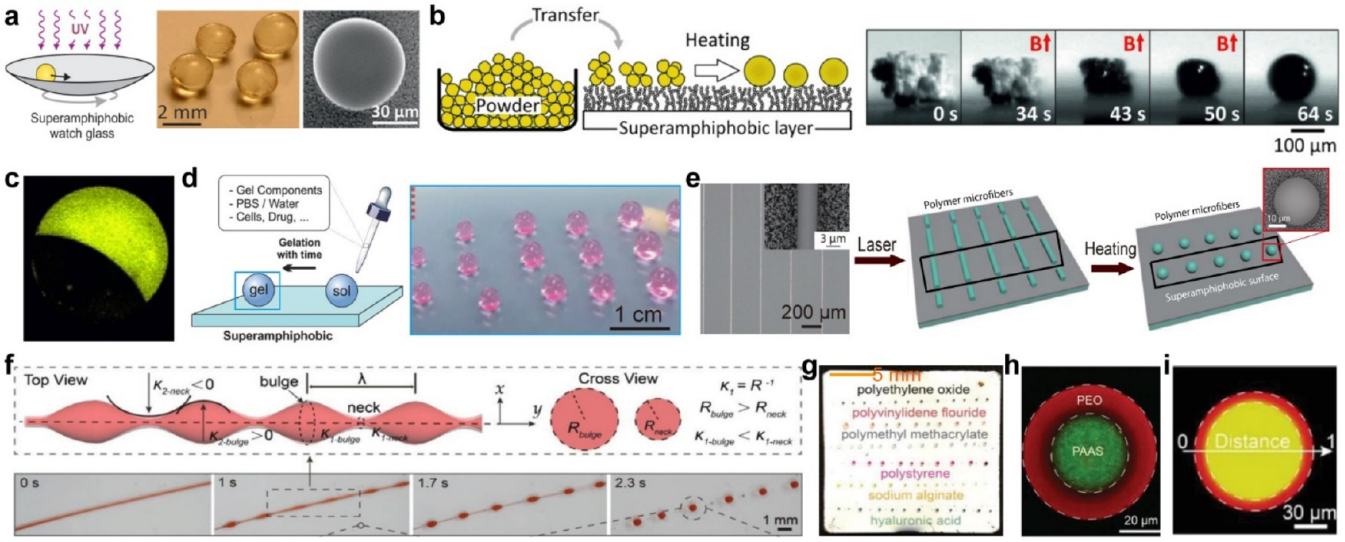

Figure 8. Synthesis of microspheres based on the high liquid repellency of the superamphiphobic surface. (a) Synthesis of microspheres by radical polymerization of a methacrylate initiated by UV light on a superamphiphobic watch glass. (b) Generation of the magnetic hybrid microspheres by heating a thermoplastic polystyrene/iron oxide composite powder on a superamphiphobic surface. (c) Janus microspheres from polystyrene and poly(methyl methacrylate) (PMMA) on a superamphiphobic surface. (d) Generating process of the gel beads/particles on a superamphiphobic surface. (e) PMMA microspheres fabricated by microfiber processing on a superamphiphobic surface. (f) Poly(ethylene oxide) (PEO) microdroplet formation from a cylindrical column via the Plateau–Rayleigh instability (PRI) on a superamphiphobic surface. (g) Wide variety of polymeric particles produced via confinement-free PRI. (h) Core–shell (PAAS-core/PEO-shell) particles fabrication. (i) Soft microcapsule (glycerol-core/Ca-Alg-shell) production. (a–c) Reproduced with permission from ref 45. Copyright 2013 John Wiley and Sons. (d) Reproduced with permission from ref 46. Copyright 2018 John Wiley and Sons. (e) Reproduced with permission from ref 47. Copyright 2020 Springer Nature. (f–i) Reproduced with permission from ref 48. Copyright 2021 John Wiley and Sons.

charge on the wettability of the superamphiphobic surface was verified by the variation curves of the contact line (Figure 6g) and dynamic CA (Figure 6h) between the liquid and the surface during the impact process. The printing of the surface charge via drop impact can be a versatile platform for potential applications, such as drop transportation and self-assembly.[40]

3. FUNCTIONAL STABILITY OF SUPER-REPELLENT SURFACES TOWARD APPLICATIONS

Super-repellent surfaces have displayed various potential applications because of their outstanding performance in liquid repulsion. However, their minimized contact area leads to a fragile surface property that hinders its application in real-world problems. Various approaches have been investigated to address the stability of liquid-repellent surfaces, including mechanical stability, chemical stability, and thermal stability.[20,41,42] Among them, the chemical and thermal stabilities of the super-repellent surface can be addressed by altering the substrate materials and preparation processes. However, the mechanical stability is determined by the inherent fragility of the micronanostructure. Therefore, the mechanical stability is the most important factor that restricts the long-term material usage. In practical application scenarios, potential friction and wear commonly exist during transportation, installation, and use of the material surfaces. The design of a super-repellent surface that withstands abrasion is a major challenge because of the fragile surface textures (essential characteristic) that exist in the rough super-repellent surface, which is highly susceptible to abrasion. Abrasion will destroy the micronano structure, expose underlying materials, and therefore lead to a failure of the liquid repellency. In line with the Cassie–Baxter equation, the solid–liquid contact area minimization contributes to the surface super-repellency. However, when the solid–liquid contact area is decreased significantly, the texture is bound to bear a higher local pressure under an external mechanical load, which makes the structure more prone to damage. This means that mechanical robustness and liquid repellency are mutually exclusive surface properties.[41,43] Therefore, the mechanical instability is the primary bottleneck that restricts the development and application of interfacial materials.

To resolve the mechanical stability problem, a design concept of decoupled superhydrophobic surfaces was recommended. The robust superhydrophobicity was achieved by structuring the surfaces at two different length scales, with a nanostructure design to provide water repellency and a microstructure design to provide durability,[41,44] as shown in Figure 7a. Combined with the wettability theory and an analysis of the mechanical mechanics principle, the microstructure was designed as an interconnected surface frame that contained pockets. Such a successive frame acts as armor to protect the water repellency and mechanically fragile nanostructures that are housed in the pockets (Figure 7b,c). For the inverted-pyramidal microstructure as an example, compared with the pillar and pyramidal discrete microstructures, the inverted-pyramidal microstructure can resist the highest load tested and experience only minor damage, as shown in Figure 7d. The resulting armored superhydrophobic surface can protect the nanostructures from abrasion and wear effectively and achieve a superhydrophobicity (Figure 7e–g), high strength, and long-term durability (Figure 7h–j). The robust superhydrophobic surface design concept has good universality and can be applied to silicon wafers, ceramics, metals, and glass substrates. The armored superhydrophobic surface integrates the resistance properties of chemical corrosion, thermal degradation, high-speed jet impact, and condensation failure. This design and manufacturing strategy demonstrates great potential and promotes the application of

https://doi.org/10.1021/accountsmr.1c00147
Acc. Mater. Res. 2021, 2, 920–932

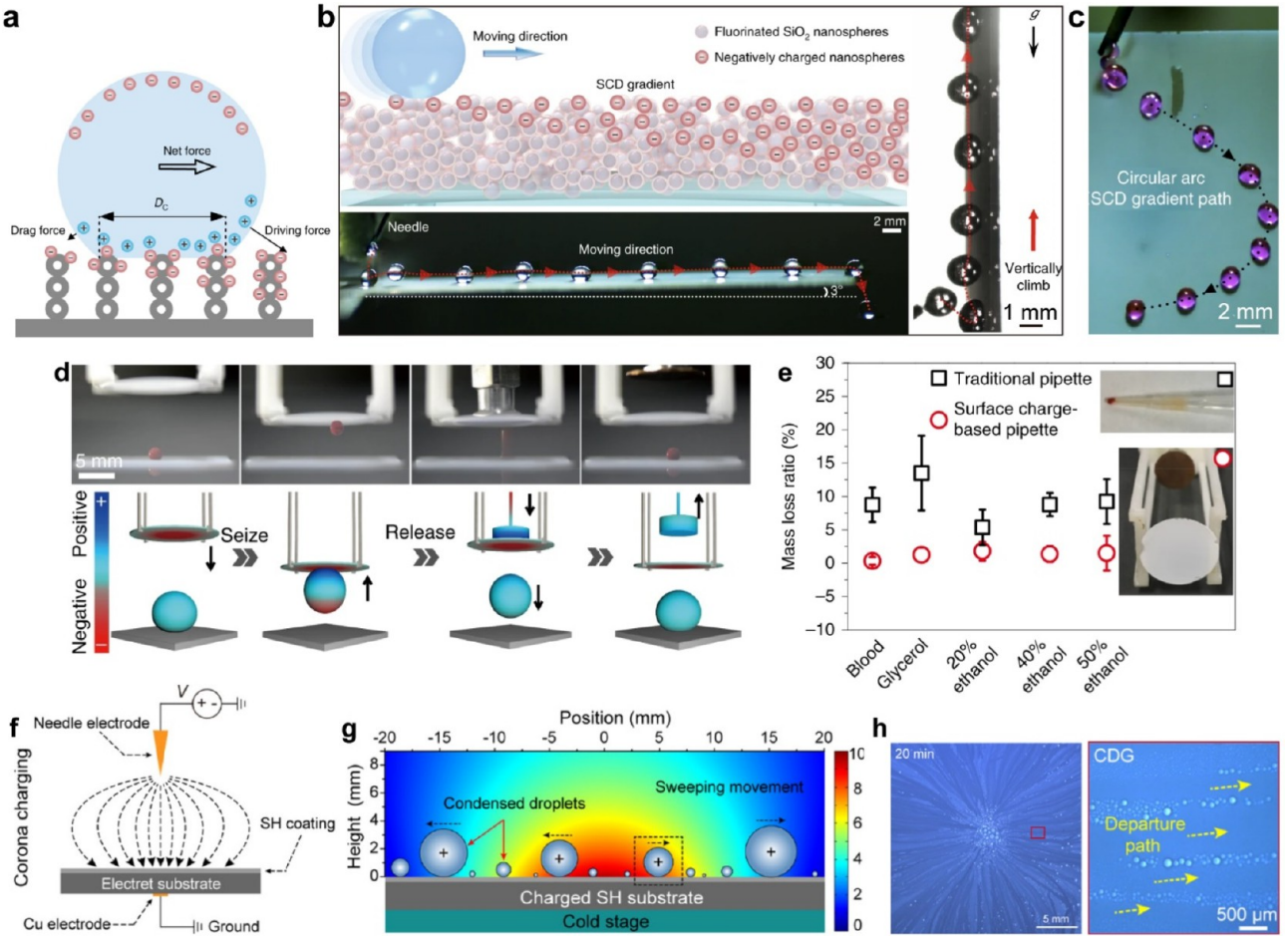

Figure 9. Drop transportation and manipulation based on the surface charge accumulation effect of the superamphiphobic surface. (a) Schematic diagram showing the mechanism of drop transportation on a superamphiphobic surface with a surface charge density gradient. (b) Drop self-propulsion on a superamphiphobic surface including climbing and upward movement. (c) The circular arc drop transportation for a particular path decorated with the surface charge density gradient. (d) Drop manipulation by a charged superamphiphobic-surface-based pipet. (e) Transfer of various liquid with extremely low mass loss by the charged surface-based pipet. (f–h) Fast transportation of condensation droplet driven by the charge density gradient. (a–e) Reproduced with permission from ref 38. Copyright 2019 Springer Nature. (f–h) Reproduced with permission from ref 52. Copyright 2021 American Chemical Society.

superhydrophobic surfaces to a wide range of practical applications.

4. APPLICATIONS

With the increasing demand for functional materials with excellent liquid repellency, the development of super-repellent surfaces with wide application prospects has become the focus of scientists. Some applications of super-repellent surfaces, such as the synthesis of microspheres, droplet transport and control, and self-cleaning solar cells, will be discussed in the following sections. These applications generally require us to integrate the robust low-adhesion property and functional stability of super-repellent surfaces.

4.1. Polymer Microsphere Synthesis

Polymer microspheres are promising candidates for a variety of applications, such as drug delivery, photonics, and smart displays, and have stimulated a number of synthesis strategies including dispersion, emulsion, and microfluidics. However, the solvent dependence or processing liquid in these methods limits the fabrication of polymer microspheres, such as yield, size control, environmental reasons, and energy consumption. A better solution may be a template-free method without solvent or processing liquid. A superamphiphobic surface, which possesses an ultralow solid–liquid fraction when in contact with low-surface-energy organic liquids and high-viscosity polymer solution, turns into a promising candidate to ball the polymer drop. As shown Figure 8a, microspheres were produced by solvent-free radical polymerization on the candle-soot-templated superamphiphobic surface.[45] Such a strategy can be extended to produce microspheres by melting a thermoplastic polymer powder because of the thermal stability of the candle-soot-templated superamphiphobic surface (Figure 8b). In a similar way, Janus microspheres from a polystyrene and poly(methyl methacrylate) blend were produced by annealing at 160 °C on the superamphiphobic surfaces (Figure 8c). Surfactant-free and shape-controllable hydrogel beads can be prepared on the superamphiphobic layer by simple drop deposition on the surface, which makes use of the nearly contact-free solid–liquid interface (Figure 8d).[46]

By combining the excellent liquid-repellency performance of the superamphiphobic surface with interfacial engineering, a multifunctional synthesis platform of polymer microspheres was established.[47] Polymer microspheres with uniform size, composition, and surface properties can be produced readily from microfibers on superamphiphobic surfaces by a deposit–

https://doi.org/10.1021/accountsmr.1c00147
Acc. Mater. Res. 2021, 2, 920–932

cut−anneal process (Figure 8e). By taking advantage of the microfluidic spinning and laser cutting, patterned microfibers with a controlled length were obtained on superamphiphobic surfaces first. Then the microfibers were shaped into microspheres because of the interfacial tension during annealing. The resulting polymer microsphere size is uniform and changes from 10 μm to the capillary length of the polymer melt. On this basis, a strategy that uses a spontaneous confinement-free Rayleigh instability of polymer solution columns on the superamphiphobic surface was developed (Figure 8f).[48] Ultrafast polymer microdroplets can be formed in this way at ambient temperature, which is friendly to thermally intolerable materials. The polymer microdroplets were evolved into polymer microspheres via in situ evaporation or cross-linking. This method can be applied to obtain a variety of polymer microspheres from 1 μm to 1 mm (Figure 8g). Composite/structured micromaterials can be produced through a simple modification of the feed solution configuration, for example, the core−shell particles and microcapsules, as shown in Figure 8h,i, respectively.

4.2. Drop Transportation and Manipulation

Drop/liquid transportation has been exploited extensively in industrial fields from water harvesting to bioanalysis. Conventional methods, such as the creation of topographic, surface-wetting gradients and a photoinduced capillary force to achieve directional drop transport, face a trade-off between the transport velocity and distance.[49,50] A long transport distance requires a relatively small wetting gradient, whereas a large wetting gradient is desired for a high transport velocity. It remains challenging to achieve long-distance and rapid drop transportation. By engineering a special superamphiphobic surface with a surface charge density gradient (Figure 9a), a drop can move spontaneously and be characterized directionally by a high transport velocity and an ultralong transport distance (Figure 9b).[38] Compared to drop transportation induced by a wetting or structure gradient and the Leidenfrost effect, the maximum transport velocity in this unique way is up to 1.1 m/s, which is more than 10 times higher than those conventional transport velocities. Such self-drive drops can also climb up a vertically placed superamphiphobic surface (Figure 9b). By taking advantage of this facile method to print a surface charge density gradient, well-programmed drop transportation can be achieved (Figure 9c). A superamphiphobic surface with a surface charge density can also be used as an opening platform to manipulate and transfer various liquid drops with an extremely low mass loss, as shown in Figure 9d,e. Inspired by the surface charge separation at the solid−liquid interface on the superamphiphobic surface, a device for obtaining energy from impinging water drops was developed using the structure of the aluminum electrode on the indium tin oxide substrate with a polytetrafuoroethylene film,[51] which made a breakthrough in water energy harvesting. By creating a more stable charge density gradient from corona charging (Figure 9f), a heterogeneous electric field that was located immediately above the superamphiphobic surface (Figure 9g) was used to sweep the condensate with a small size and a high velocity.[52] The removal efficiency of the condensation microdroplets was improved significantly on the superamphiphobic surface with a surface charge density gradient in an ultrafast sweeping manner (Figure 9h).

4.3. Self-Cleaning Solar Panel

A solar panel is a unit that transforms solar radiation from sunlight into electric energy through photoelectric or photochemical effects in a direct or indirect way. Sunlight transmittance determines the energy conversion efficiency of solar cells. However, the dust and dirt in an air environment restrict the transmittance of sunlight significantly. The excellent self-cleaning property of the superhydrophobic surface has become a promising choice for maintaining the high light transmittance of solar panels.[53] Additionally, the self-cleaning surface also needs to be transparent to ensure good light transmission. Generally, the transmittance declines with an increase in surface roughness, especially when the roughness scale goes beyond the light wavelength. Therefore, the surface texture should be finely regulated. Figure 10a,b shows the transmittance and current density as a solar panel of a transparent superhydrophobic coating that is composed of porous silica capsules.[53] The transparent coating can be applied to the solar panels and ensure the energy efficiency meanwhile. The armored superhydrophobic glass surface enables a high energy-conversion efficiency to

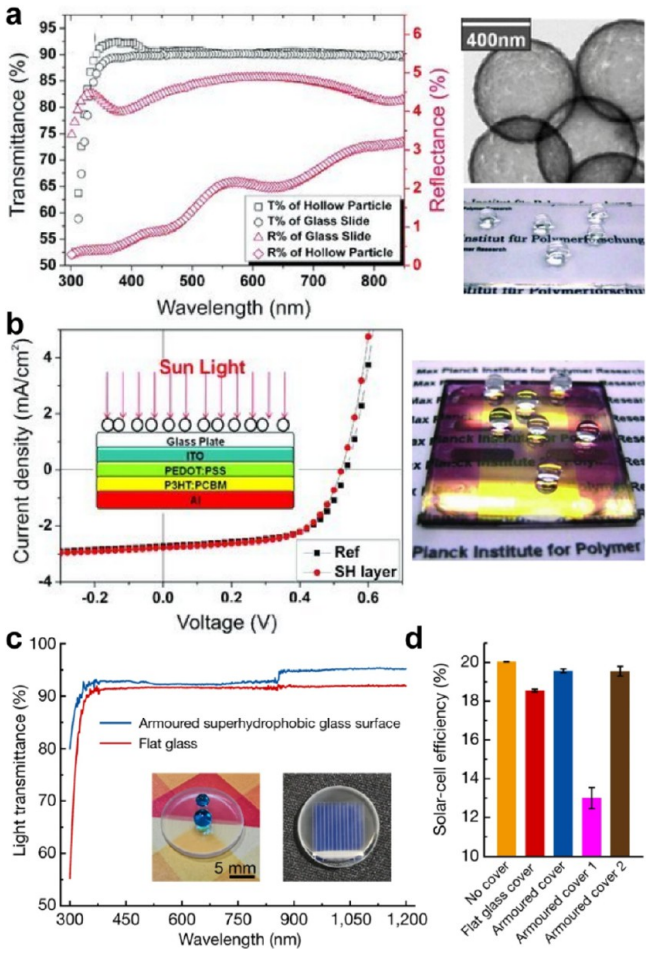

Figure 10. Solar panel efficiency enhancement based on the self-cleaning and transparent robust superamphiphobic surface. (a) Transmittance and reflectance spectra of a transparent superhydrophobic surface composed of hollow raspberry-like silica particles. (b) Current−voltage curves of organic solar cells prepared on a glass substrate. The right image shows water drops sitting on the solar cell. (c) Transmission spectra of an armored superhydrophobic glass (blue) compared to a flat glass (red). (d) Energy-conversion efficiency of the solar panel with the armored superhydrophobic structures or not. (a, b) Reproduced with permission from ref 53. Copyright 2011 John Wiley and Sons. (c, d) Reproduced with permission from ref 41. Copyright 2020 Springer Nature.

https://doi.org/10.1021/accountsmr.1c00147
Acc. Mater. Res. 2021, 2, 920−932

be maintained when it serves as the topcoat for solar cells as shown in Figure 10c,d.[41] Meanwhile, from the nonwettability and optical transparency, such armored surfaces also possess mechanical robustness, which provides a great advantage in applications.

5. CONCLUSIONS AND PERSPECTIVE

In this Account, we summarized our recent progress in super-repellent surfaces, mainly focusing on the structure design, wetting mechanism, functional stability, and applications from the perspective of durability. By elaborating the control of solid−liquid interaction, we have achieved super-repellent materials with a highly stable Cassie−Baxter state. We then discussed the shortage of super-repellent materials in real-world applications and a resolution to the problem. On this basis, we highlighted the potential for the application of super-repellent materials in a broad range of areas, such as microsphere synesis, drop transportation, and solar panels.

Although there have been excellent achievements in super-repellent functional materials, challenges remain in other key problems in the applications of the material themselves, such as the performance to resist failure in long-term condensation and the ability for antiultraviolet aging and weather resistance outdoors. The achievement of the large-scale industrial application of super-repellent materials that is independent of the substrate and controls research costs is an important future direction. Problematic large-scale preparation and optimized processes and technologies should be exploited to control the cost and extend the liquid-repellent material to a wide range of applications. On the basis of the complexity of applications in processing, an enabling of materials with multiple functions is a promising strategy. Finally, prospective applications of intelligent, regulated, multifunctional liquid-repellent materials, such as military, biomedical, oceanic, electronics, energy, and other innovative fields, should be explored.

AUTHOR INFORMATION

Corresponding Author

Xu Deng − *Center for Materials Surface Science, Institute of Fundamental and Frontier Sciences, University of Electronic Science and Technology of China, Chengdu 610054, P. R. China;* orcid.org/0000-0002-9659-0417; Email: dengxu@uestc.edu.cn

Authors

Fanfei Yu − *Center for Materials Surface Science, Institute of Fundamental and Frontier Sciences, University of Electronic Science and Technology of China, Chengdu 610054, P. R. China; Yangtze Delta Region Institute (Huzhou), University of Electronic Science and Technology of China, Huzhou 313001, P. R. China*

Dehui Wang − *Center for Materials Surface Science, Institute of Fundamental and Frontier Sciences, University of Electronic Science and Technology of China, Chengdu 610054, P. R. China; Yangtze Delta Region Institute (Huzhou), University of Electronic Science and Technology of China, Huzhou 313001, P. R. China*

Jinlong Yang − *Center for Materials Surface Science, Institute of Fundamental and Frontier Sciences, University of Electronic Science and Technology of China, Chengdu 610054, P. R. China; Institute for Advanced Study, Chengdu University, Chengdu 610106, P. R. China*

Wenluan Zhang − *Center for Materials Surface Science, Institute of Fundamental and Frontier Sciences, University of Electronic Science and Technology of China, Chengdu 610054, P. R. China;* orcid.org/0000-0001-5651-7314

Complete contact information is available at: https://pubs.acs.org/10.1021/accountsmr.1c00147

Notes

The authors declare no competing financial interest.

Biographies

Fanfei Yu obtained her Ph.D. in materials science and engineering in 2021, supervised by Prof. Xu Deng at the University of Electronic Science and Technology of China. Her research interests center on the solid−liquid interface interactions of superwetting materials, including the investigation of the phenomenon and dynamic wettability during drop impact and the corresponding applications.

Dehui Wang obtained his Ph.D. degree in materials science and engineering in 2020 from the University of Electronic Science and Technology of China (Chengdu, China) under the supervision of Prof. Xu Deng. He has been a professor of Materials Science and Engineering at the University of Electronic Science and Technology of China, and his research interests include the chemistry and physics of material surfaces and their applications to waterproofing, anti-icing, and heat-transfer enhancement.

Jinlong Yang is currently a postdoctoral fellow from the University of Electric Science and Technology of China. He received his Ph.D. degree in 2017 from the University of Hawaii at Manoa. His research interests focus on the wettability, solid−liquid interaction, and self-assembly of colloids.

Wenluan Zhang received his bachelor's degree in materials science from the University of Science and Technology of China (Hefei, China) in 2009. Then he received a Ph.D. in materials science and engineering from the University of Delaware (U.S.A.). In 2017, he joined the University of Electronic Science and Technology of China as an assistant professor. His current research interests lie in the physical chemistry of interfaces, novel forms of energy conversion, and the application of nanomaterials to sustainable development.

Xu Deng received his Ph.D. in 2013 from the Max Planck Institute for Polymer Research. In 2014, Dr. Deng served as a postdoctoral fellow at UC Berkeley and Lawrence Berkeley National Laboratory. In 2017, he was pointed by the president of the Max Planck Institute as the head of Max Planck Partner Group at UESTC. Dr. Deng is interested in understanding wetting dynamics and physical chemistry at interfaces. He has published more than 50 articles as the first author or corresponding author in leading journals such as *Science*, *Nature*, *Nature Materials*, *Physical Review Letters*, *Angewandte Chemie*, and *Advanced Materials*, to name a few.

ACKNOWLEDGMENTS

We acknowledge funding support by the National Natural Science Foundation of China (22072014), the Fundamental Research Funds for the Central Universities (ZYGX2019J119), Max-Planck-Gesellschaft (Max Plank Partner Group UESTC-MPIP), the Sichuan Science and Technology Program (2021JDRC0016), and the Sichuan Outstanding Young Scholars Foundation (21JCQN0235).

REFERENCES

(1) Feng, L.; Li, S. H.; Li, Y. S.; Li, H. J.; Zhang, L. J.; Zhai, J.; Song, Y. L.; Liu, B. Q.; Jiang, L.; Zhu, D. B. Super-Hydrophobic Surfaces: From Natural to Artificial. *Adv. Mater.* **2002**, *14*, 1857−1860.

(2) Wisdom, K. M.; Watson, J. A.; Qu, X. P.; Liu, F. J.; Watson, G. S.; Chen, C. H. Self-Cleaning of Superhydrophobic Surfaces by Self-Propelled Jumping Condensate. *Proc. Natl. Acad. Sci. U. S. A.* **2013**, *110*, 7992−7997.

(3) Mouterde, T.; Lehoucq, G.; Xavier, S.; Checco, A.; Black, C. T.; Rahman, A.; Midavaine, T.; Clanet, C.; Quere, D. Antifogging Abilities of Model Nanotextures. *Nat. Mater.* **2017**, *16*, 658−663.

(4) Zhang, S. N.; Huang, J. Y.; Cheng, Y.; Yang, H.; Chen, Z.; Lai, Y. K. Bioinspired Surfaces with Superwettability for Anti-Icing and Ice-Phobic Application: Concept, Mechanism, and Design. *Small* **2017**, *13*, 2.

(5) Golovin, K.; Dhyani, A.; Thouless, M. D.; Tuteja, A. Low-Interfacial Toughness Materials for Effective Large-Scale Deicing. *Science* **2019**, *364*, 371−375.

(6) Wang, B.; Liang, W. X.; Guo, Z. G.; Liu, W. M. Biomimetic Super-lyophobic and Super-lyophilic Materials Applied for Oil/Water Separation: A New Strategy Beyond Nature. *Chem. Soc. Rev.* **2015**, *44*, 336−361.

(7) Lee, C.; Kim, C. J. Underwater Restoration and Retention of Gases on Superhydrophobic Surfaces for Drag Reduction. *Phys. Rev. Lett.* **2011**, *106*, 014502.

(8) Bhushan, B.; Jung, Y. C. Natural and Biomimetic Artificial Surfaces for Superhydrophobicity, Self-Cleaning, Low Adhesion, and Drag Reduction. *Prog. Mater. Sci.* **2011**, *56*, 1−108.

(9) Liu, M. J.; Wang, S. T.; Jiang, L. Nature-Inspired Superwettability Systems. *Nat. Rev. Mater.* **2017**, *2*, 17036.

(10) Barthlott, W.; Neinhuis, C. Purity of the Sacred Lotus, or Escape from Contamination in Biological Surfaces. *Planta* **1997**, *202*, 1−8.

(11) Gao, X. F.; Jiang, L. Water-Repellent Legs of Water Striders. *Nature* **2004**, *432*, 36−36.

(12) Parker, A. R.; Lawrence, C. R. Water Capture by a Desert Beetle. *Nature* **2001**, *414*, 33−34.

(13) Pan, S. J.; Guo, R.; Bjornmalm, M.; Richardson, J. J.; Li, L.; Peng, C.; Bertleff-Zieschang, N.; Xu, W. J.; Jiang, J. H.; Caruso, F. Coatings Super-Repellent to Ultralow Surface Tension Liquids. *Nat. Mater.* **2018**, *17*, 1040−1047.

(14) Peng, C. Y.; Chen, Z. Y.; Tiwari, M. K. All-Organic Superhydrophobic Coatings with Mechanochemical Robustness and Liquid Impalement Resistance. *Nat. Mater.* **2018**, *17*, 355−360.

(15) Genzer, J.; Efimenko, K. Creating Long-Lived Superhydrophobic Polymer Surfaces Through Mechanically Assembled Monolayers. *Science* **2000**, *290*, 2130−2133.

(16) Lu, Y.; Sathasivam, S.; Song, J. L.; Crick, C. R.; Carmalt, C. J.; Parkin, I. P. Robust Self-Cleaning Surfaces That Function When Exposed to Either Air or Oil. *Science* **2015**, *347*, 1132−1135.

(17) Tian, X. L.; Verho, T.; Ras, R. H. A. Moving Superhydrophobic Surfaces Toward Real-World Applications. *Science* **2016**, *352*, 142−143.

(18) Tuteja, A.; Choi, W.; Ma, M. L.; Mabry, J. M.; Mazzella, S. A.; Rutledge, G. C.; McKinley, G. H.; Cohen, R. E. Designing Superoleophobic Surfaces. *Science* **2007**, *318*, 1618−1622.

(19) Jing, X. S.; Guo, Z. G. Biomimetic Super Durable and Stable Surfaces with Superhydrophobicity. *J. Mater. Chem. A* **2018**, *6*, 16731−16768.

(20) Deng, X.; Mammen, L.; Butt, H. J.; Vollmer, D. Candle Soot as a Template for a Transparent Robust Superamphiphobic Coating. *Science* **2012**, *335*, 67−70.

(21) Qing, Y. Q.; Shi, S. L.; Lv, C. J.; Zheng, Q. S. Microskeleton-Nanofiller Composite with Mechanical Super-Robust Superhydrophobicity against Abrasion and Impact. *Adv. Funct. Mater.* **2020**, *30*, 1910665.

(22) Young, T. An Essay on The Cohesion of Fluids. *Philos. Trans.* **1805**, *95*, 65−87.

(23) Wenzel, R. N. Resistance of Solid Surfaces to Wetting by Water. *Ind. Eng. Chem.* **1936**, *28*, 988−994.

(24) Cassie, A.; Baxter, S. Wettability of Porous Surfaces. *Trans. Faraday Soc.* **1944**, *40*, 546−551.

(25) Tuteja, A.; Choi, W. J.; McKinley, G. H.; Cohen, R. E.; Rubner, M. F. Design Parameters for Superhydrophobicity and Super-oleophobicity. *MRS Bull.* **2008**, *33*, 752−758.

(26) Sarma, J.; Guo, Z. Q.; Dai, X. M. Bioinspired Photocatalytic Hedgehog Coating for Super Liquid Repellency. *Mater. Chem. Front.* **2021**, *5*, 4174−4181.

(27) Li, X.; Wang, D.; Tan, Y.; Yang, J.; Deng, X. Designing Transparent Micro/Nano Re-Entrant-Coordinated Superamphiphobic Surfaces with Ultralow Solid/Liquid Adhesion. *ACS Appl. Mater. Interfaces* **2019**, *11*, 29458−29465.

(28) Sun, J.; Zhu, P.; Yan, X.; Zhang, C.; Jin, Y.; Chen, X.; Wang, Z. J. A. P. R. Robust Liquid Repellency by Stepwise Wetting Resistance. *Appl. Phys. Rev.* **2021**, *8*, 031403.

(29) Papadopoulos, P.; Mammen, L.; Deng, X.; Vollmer, D.; Butt, H. J. How Superhydrophobicity Breaks Down. *Proc. Natl. Acad. Sci. U. S. A.* **2013**, *110*, 3254−3258.

(30) Ye, M.; Deng, X.; Ally, J.; Papadopoulos, P.; Schellenberger, F.; Vollmer, D.; Kappl, M.; Butt, H. J. Superamphiphobic Particles: How Small Can We Go? *Phys. Rev. Lett.* **2014**, *112*, 016101.

(31) Whyman, G.; Bormashenko, E. How to Make the Cassie Wetting State Stable? *Langmuir* **2011**, *27*, 8171−8176.

(32) Li, Y. S.; Quere, D.; Lv, C. J.; Zheng, Q. S. Monostable Superrepellent Materials. *Proc. Natl. Acad. Sci. U. S. A.* **2017**, *114*, 3387−3392.

(33) Li, X.; Yang, J.; Lv, K.; Papadopoulos, P.; Sun, J.; Wang, D.; Zhao, Y.; Chen, L.; Wang, D.; Wang, Z.; Deng, X. Salvinia-Like Slippery Surface with Stable and Mobile Water/Air Contact Line. *Natl. Sci. Rev.* **2021**, *8*, nwaa153.

(34) Jung, Y. C.; Bhushan, B. Dynamic Effects Induced Transition of Droplets on Biomimetic Superhydrophobic Surfaces. *Langmuir* **2009**, *25*, 9208−9218.

(35) Deng, X.; Schellenberger, F.; Papadopoulos, P.; Vollmer, D.; Butt, H. J. Liquid Drops Impacting Superamphiphobic Coatings. *Langmuir* **2013**, *29*, 7847−7856.

(36) Zhao, B.; Wang, X.; Zhang, K.; Chen, L.; Deng, X. Impact of Viscous Droplets on Superamphiphobic Surfaces. *Langmuir* **2017**, *33*, 144−151.

(37) Yu, F.; Lin, S.; Yang, J.; Fan, Y.; Wang, D.; Chen, L.; Deng, X. Prompting Splash Impact on Superamphiphobic Surfaces by Imposing a Viscous Part. *Adv. Sci. (Weinh)* **2020**, *7*, 1902687.

(38) Sun, Q.; Wang, D.; Li, Y.; Zhang, J.; Ye, S.; Cui, J.; Chen, L.; Wang, Z.; Butt, H. J.; Vollmer, D.; Deng, X. Surface Charge Printing for Programmed Droplet Transport. *Nat. Mater.* **2019**, *18*, 936−941.

(39) Yu, F.; Sun, Q.; Wang, D.; Tan, Y.; Lin, S.; Chen, L.; Fan, Y.; Guo, J.; Yang, J.; Deng, X. Surface-Charge-Assisted Microdroplet Generation on a Superhydrophobic Surface. *Langmuir* **2020**, *36*, 14352−14360.

(40) Zhang, W. L.; Sun, Q. Q.; Butt, H. J.; Wang, Z. K.; Deng, X. Surface Charges as a Versatile Platform for Emerging Applications. *Sci. Bull.* **2020**, *65*, 1052−1054.

(41) Wang, D.; Sun, Q.; Hokkanen, M. J.; Zhang, C.; Lin, F. Y.; Liu, Q.; Zhu, S. P.; Zhou, T.; Chang, Q.; He, B.; Zhou, Q.; Chen, L.; Wang, Z.; Ras, R. H. A.; Deng, X. Design of Robust Superhydrophobic Surfaces. *Nature* **2020**, *582*, 55−59.

(42) Zhang, L.; Guo, Z.; Sarma, J.; Dai, X. Passive Removal of Highly Wetting Liquids and Ice on Quasi-Liquid Surfaces. *ACS Appl. Mater. Interfaces* **2020**, *12*, 20084−20095.

(43) Zhang, W.; Wang, D.; Sun, Z.; Song, J.; Deng, X. Robust Superhydrophobicity: Mechanisms and Strategies. *Chem. Soc. Rev.* **2021**, *50*, 4031−4061.

(44) Groten, J.; Ruhe, J. Surfaces with Combined Microscale and Nanoscale Structures: A Route to Mechanically Stable Superhydrophobic Surfaces? *Langmuir* **2013**, *29*, 3765−3772.

(45) Deng, X.; Paven, M.; Papadopoulos, P.; Ye, M.; Wu, S.; Schuster, T.; Klapper, M.; Vollmer, D.; Butt, H. J. Solvent-Free Synthesis of Microparticles on Superamphiphobic Surfaces. *Angew. Chem., Int. Ed.* **2013**, *52*, 11286−11289.

https://doi.org/10.1021/accountsmr.1c00147
Acc. Mater. Res. 2021, 2, 920−932

(46) Schlaich, C.; Fan, Y.; Dey, P.; Cui, J.; Wei, Q.; Haag, R.; Deng, X. Universal, Surfactant-Free Preparation of Hydrogel Beads on Super-amphiphobic and Slippery Surfaces. *Adv. Mater. Interfaces* **2018**, *5*, 1701536.
(47) Fan, Y.; Wang, D.-H.; Yang, J.-L.; Song, J.-N.; Li, X.-M.; Zhang, C.-L.; Wang, D.-S.; Chen, L.-Q.; Cui, J.-X.; Deng, X. Top-down Approach for Fabrication of Polymer Microspheres by Interfacial Engineering. *Chin. J. Polym. Sci.* **2020**, *38*, 1286−1293.
(48) Song, J.; Zhang, W.; Wang, D.; Fan, Y.; Zhang, C.; Wang, D.; Chen, L.; Miao, B.; Cui, J.; Deng, X. Polymeric Microparticles Generated via Confinement-Free Fluid Instability. *Adv. Mater.* **2021**, *33*, 2007154.
(49) Daniel, S.; Chaudhury, M. K.; Chen, J. C. Fast Drop Movements Resulting from the Phase Change on a Gradient Surface. *Science* **2001**, *291*, 633−636.
(50) Chen, H. W.; Zhang, P. F.; Zhang, L. W.; Iu, H. L. L.; Jiang, Y.; Zhang, D. Y.; Han, Z. W.; Jiang, L. Continuous Directional Water Transport on the Peristome Surface of Nepenthes Alata. *Nature* **2016**, *532*, 85−89.
(51) Xu, W. H.; Zheng, H. X.; Liu, Y.; Zhou, X. F.; Zhang, C.; Song, Y. X.; Deng, X.; Leung, M.; Yang, Z. B.; Xu, R. X.; Wang, Z. L.; Zeng, X. C.; Wang, Z. K. A Droplet-Based Electricity Generator with High Instantaneous Power Density. *Nature* **2020**, *578*, 392−396.
(52) Zhang, C.; Wang, D.; Yang, J.; Zhang, W.; Sun, Q.; Yu, F.; Fan, Y.; Li, Y.; Chen, L.; Deng, X. Charge Density Gradient Propelled Ultrafast Sweeping Removal of Dropwise Condensates. *J. Phys. Chem. B* **2021**, *125*, 1936−1943.
(53) Deng, X.; Mammen, L.; Zhao, Y.; Lellig, P.; Mullen, K.; Li, C.; Butt, H. J.; Vollmer, D. Transparent, Thermally Stable and Mechanically Robust Superhydrophobic Surfaces Made from Porous Silica Capsules. *Adv. Mater.* **2011**, *23*, 2962−2965.

https://doi.org/10.1021/accountsmr.1c00147
Acc. Mater. Res. 2021, 2, 920−932